Supporting information

# Stretchable flexible fiber supercapacitors for wearable integrated devices

Yujia Chen [a, b], Huihui Jin [a, b], Jiayu Zhang [b], Qirui Wu [b], Songjiu Han [b], Anbang Chen [b], Lunhui Guan [a, b], ∗

[a] College of Chemistry, Fuzhou University, Fuzhou 350108, China

[b] State Key Laboratory of Structural Chemistry, Fujian Key Laboratory of Nanomaterials, and CAS Key Laboratory of Design and Assembly of Functional Nanostructures, Fujian Institute of Research on the Structure of Matter, Chinese Academy of Sciences, Fuzhou, Fujian 350108, China.

Keywords: Supercapacitors; Flexible sensor; Wearable integrated devices; Flexible electronic device
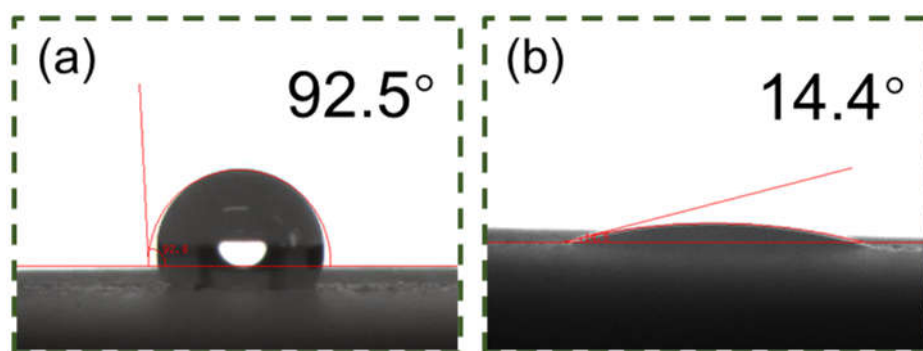
Figure S1. Contact Angle Test (a) Photomicrograph of contact angle of TPU with water droplets before plasma cleaner treatment. (b) Photomicrograph of contact angle of TPU with water droplets after plasma cleaner treatment.
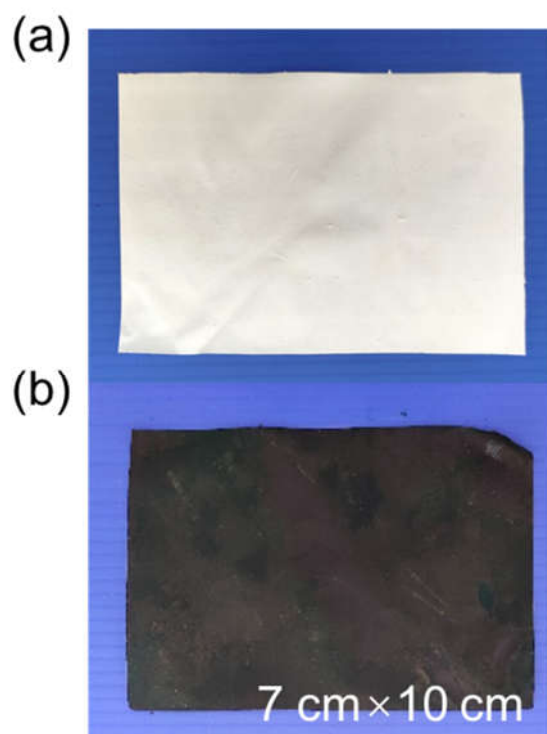
Figure S2. Optical photographs of film (a) Optical photograph of TPU. (b) Optical photograph of PANI-TPU.

PANI-TPU fiber

1 mol/L H_2SO_4

Ag/AgCl reference electrode
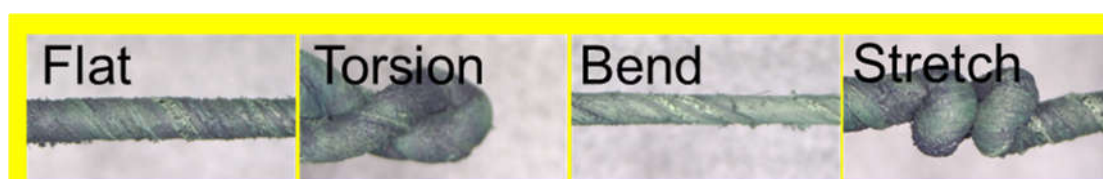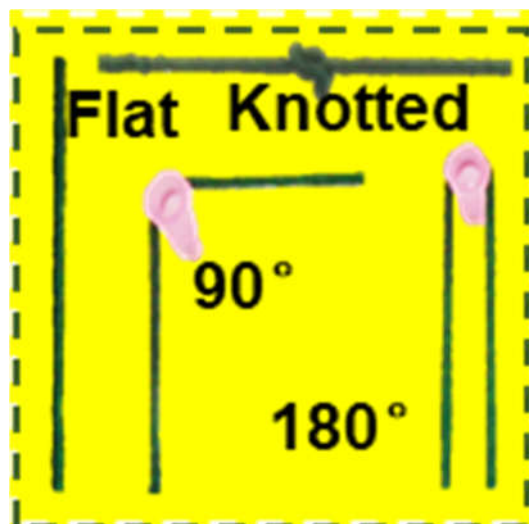
Platinum electrode
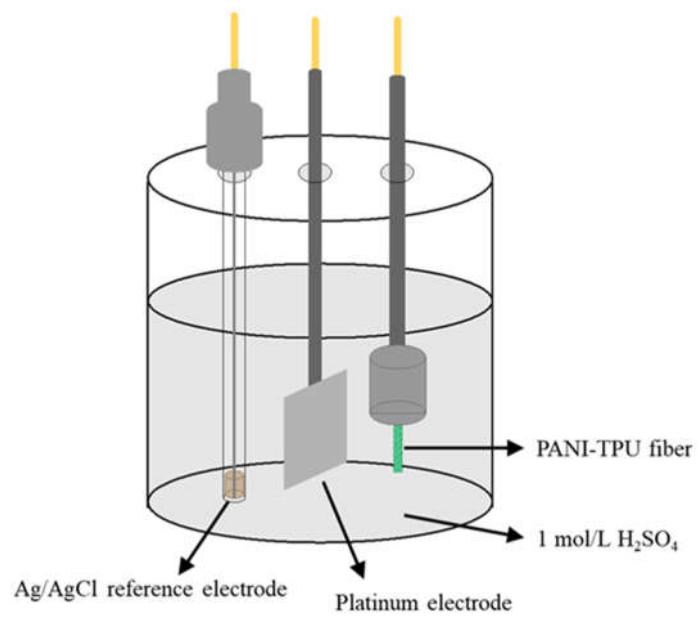
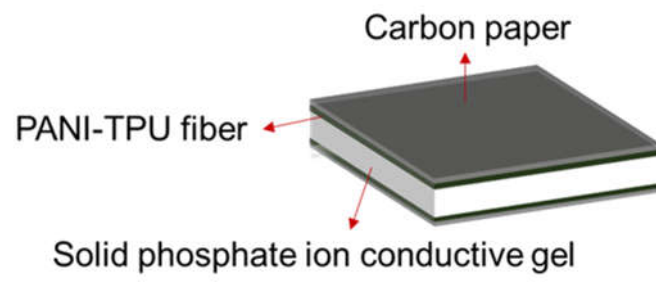**Figure S3.** Schematic diagram of the three-electrode system.
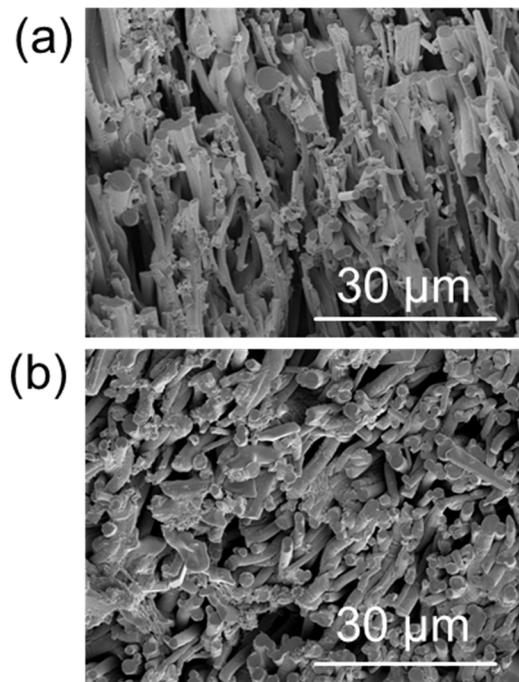
Figure S4. SEM images of dried TPU fiber and PANI-TPU fiber in section (a) SEM images of dried PANI-TPU film sections. (b) SEM images of dried PANI-TPU fiber sections.
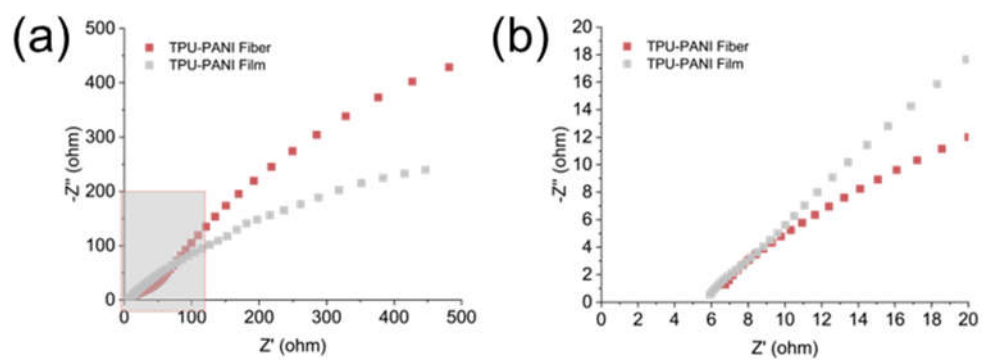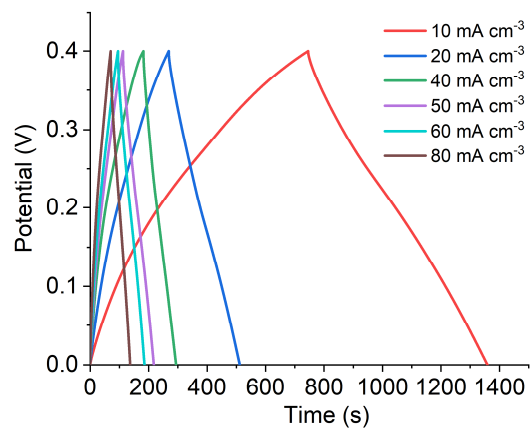
Figure S5. EIS curves of PANI-TPU film and PANI fiber.

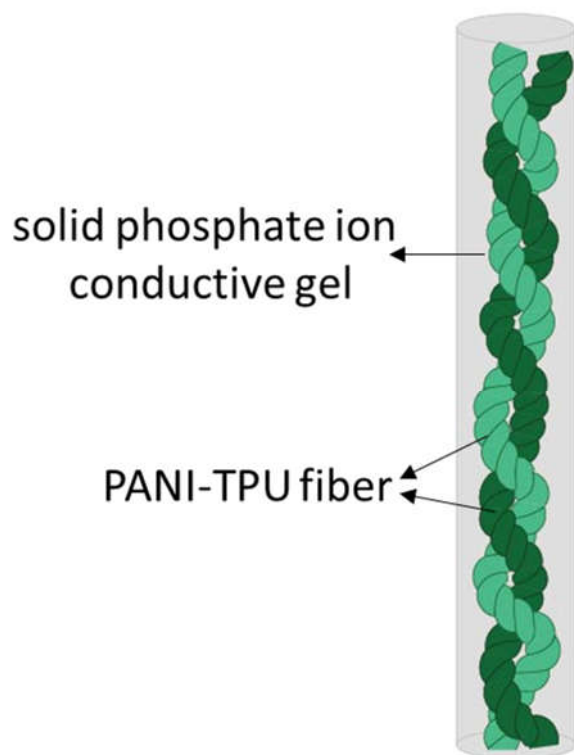**Figure S6.** Different deformations of PANI-TPU fibers.
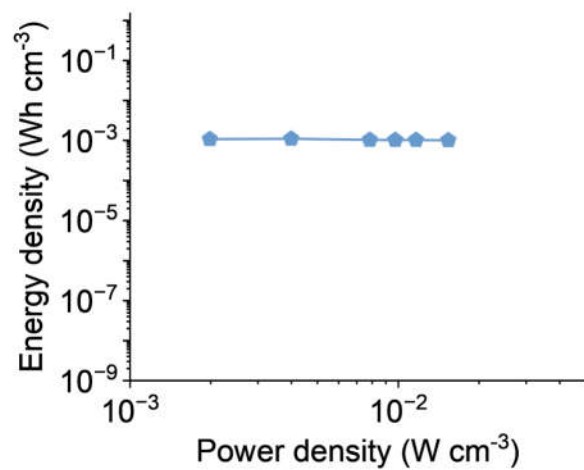
Figure S7. Sandwich structure schematic.

Figure S8. GCD curves of single PANI-TPU film supercapacitor devices at different current densities.
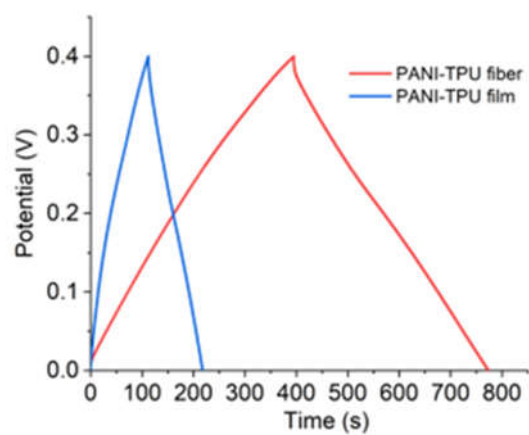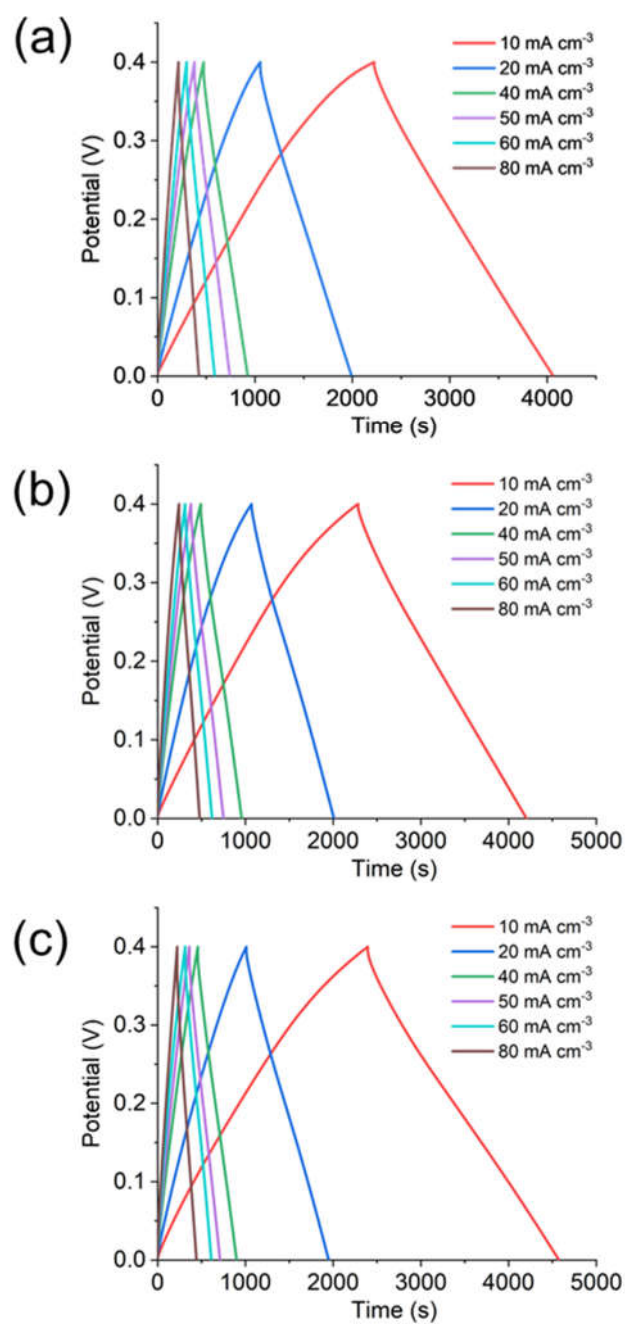
Figure S9. Schematic diagram of a single PANI-TPU fiber supercapacitor device.

Figure S10. Power density and energy density calculated from the GCD curves.

Figure S11. GCD curves of PANI-TPU membranes and PANI-TPU fiber of the same volume at a current density of 50 mA cm^{-3}.

Figure S12. GCD curves for different deformation cases. (a) GCD curves of PANI-TPU supercapacitors under 50% stretch at different current densities. (b) GCD curves of PANI-TPU supercapacitors under 90° bending at different current densities. (c) GCD curves of PANI-TPU supercapacitors in torsion at different current densities.
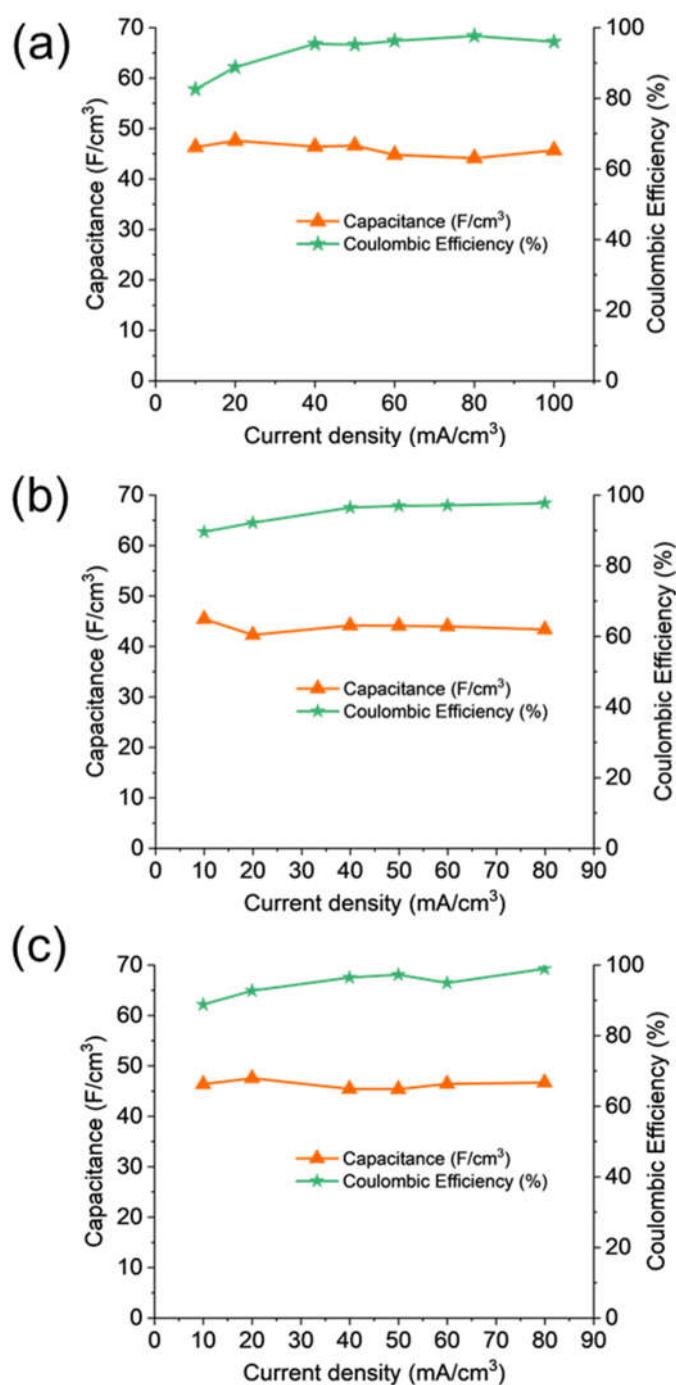
**Figure S13.** Volumetric capacitance and coulombic efficiency for different deformation cases. (a) Volumetric capacitance and coulombic efficiency of PANI-TPU supercapacitors at 50% stretch at different current densities calculated from GCD curves. (b) Volumetric capacitance and coulombic efficiency of PANI-TPU supercapacitors at different current densities under 90° bending condition calculated from GCD curves. (c) Volumetric capacitance and coulombic efficiency of PANI-TPU supercapacitors in the twisted state at different current densities were calculated from GCD curves.
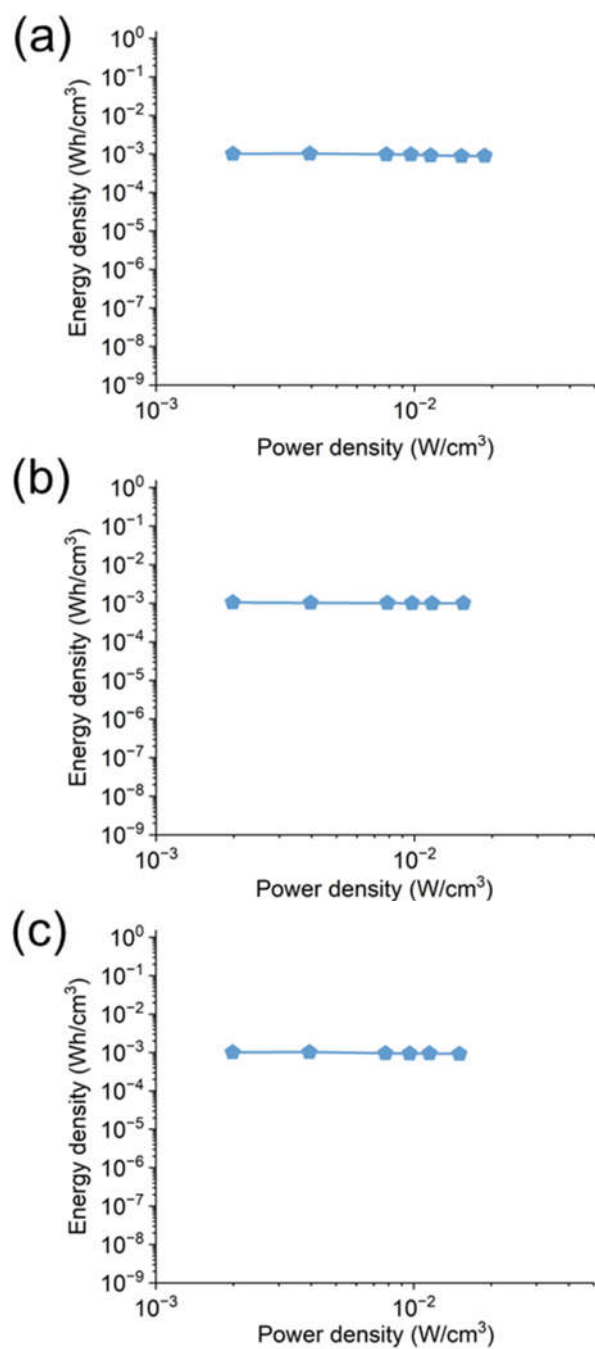
Figure S14. Power density and energy density for different deformation cases. (a) Power density and energy density under PANI-TPU supercapacitors at 50% stretch were calculated from GCD curves. (b) Power density and energy density of PANI-TPU supercapacitor in 90° bending condition calculated from GCD curve. (c) Power density and energy density of PANI-TPU supercapacitor in torsion state calculated from GCD curve.
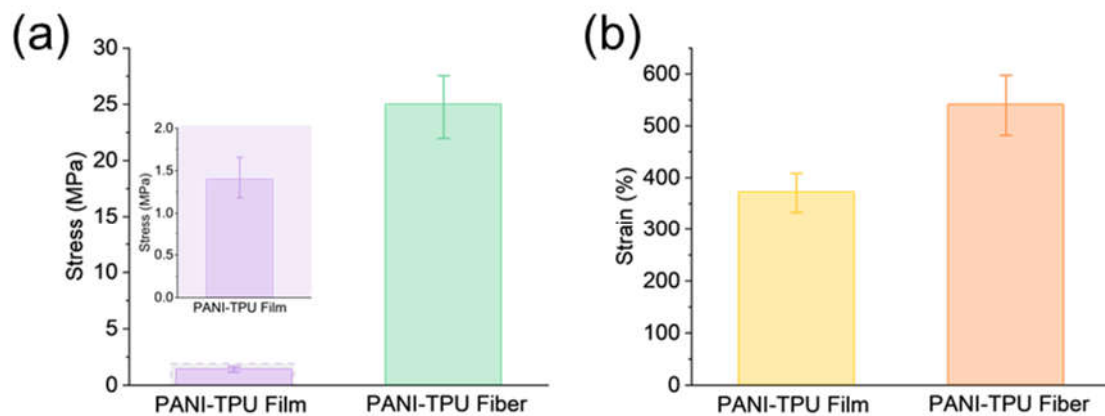
Figure S15. Stress-strain of ten independently repeated experiments. (a) Stress values of PANI-TPU membranes and PANI-TPU fiber for ten independent repetitions of the experiment. (b) Strain values of PANI-TPU membranes and PANI-TPU fiber for ten independent repetitions of the experiment.
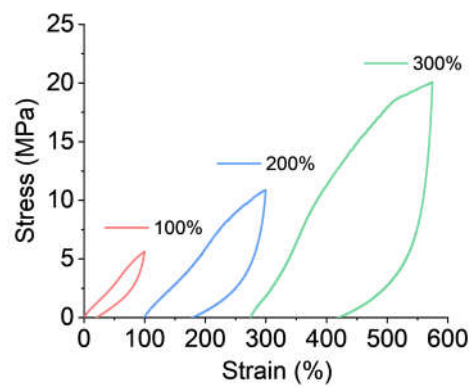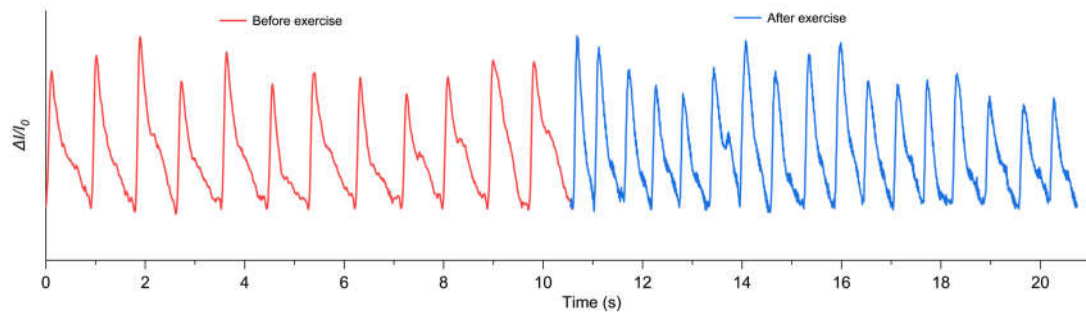
Figure S16. Stretch-shrinkage cycle curves of PANITPU fibers for a single stretching up to 100%, 200%, and 300%.
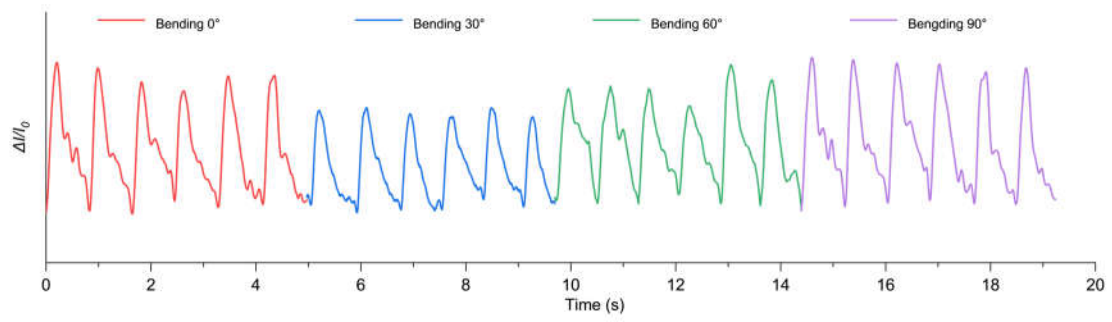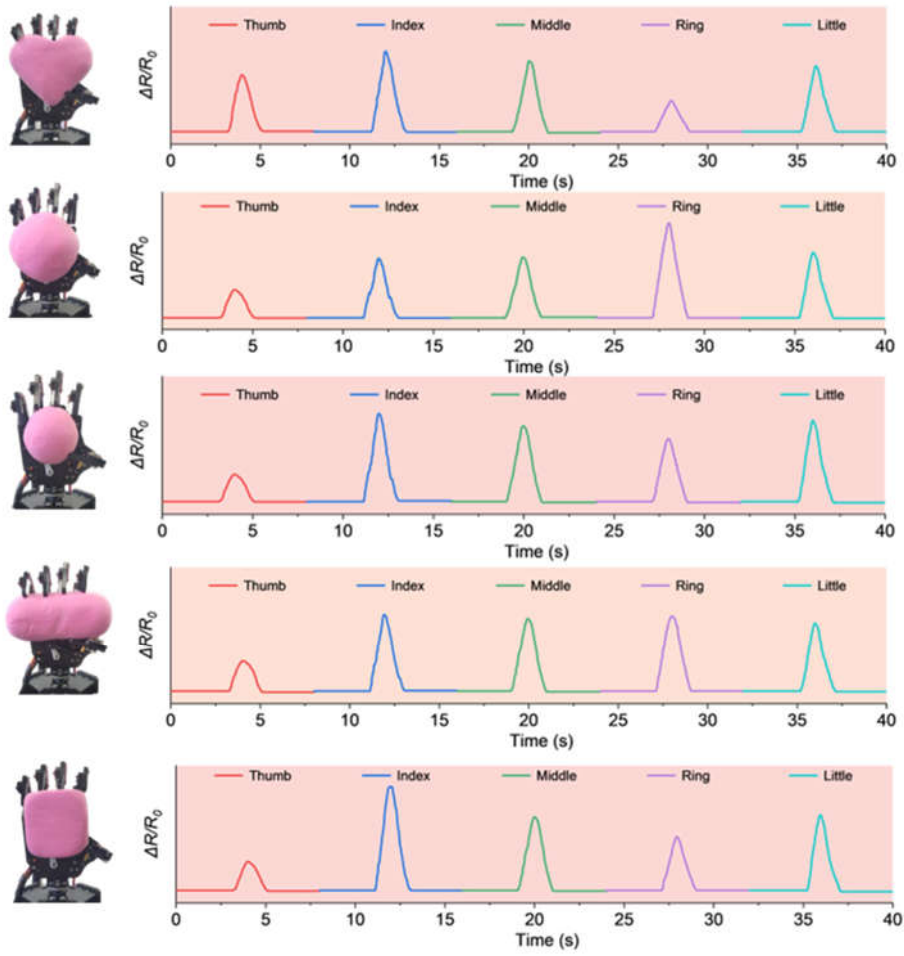
Figure S17. Self-supporting integrated sensing system for detecting pulse signals at different bending angles.

Figure S18. Self-supporting integrated sensing system for detecting pulse signals before and after exercise.

Figure S19. Self-supporting integrated sensing system for detecting signals at the hand joints when the robot grips objects of different shapes.